WATER RESOURCES RESEARCH, VOL. 35, NO. 7, PAGES 2007–2013, JULY 1999

Characterization of leaky faults: Study of air flow in faulted vadose zones

Chao Shan, Iraj Javandel, and Paul A. Witherspoon

Earth Sciences Division, Lawrence Berkeley National Laboratory, University of California, Berkeley

Abstract. Characterization of leaky faults in vadose zones of large thickness is very important for engineering problems such as high-level nuclear waste disposal. This paper presents analytical solutions for air flow in faulted vadose zones of large or small thicknesses. The focus is on those sites where the fault zone is more permeable than its adjacent rock matrix. On the basis of the assumptions of a two-dimensional air flow in the matrix and a one-dimensional air flow in the fault zone, analytical solutions are presented for a sinusoidal atmospheric pressure variation. A procedure is then provided for extending the application of the solutions to an arbitrary atmospheric pressure variation. The solutions can help determine air permeability of leaky faults in the vadose zone.

1. Introduction

A highly conductive leaky fault can provide a preferred pathway for underground fluid flow. In an engineering project with a fault on site it is very important to characterize the fault before making any design decision. For example, the presence of faults at the proposed high-level radioactive waste repository site in Yucca Mountain, Nevada, has led to concerns about the site suitability.

Movement of air in the vadose zone in response to barometric pressure changes was first described and analyzed by *Buckingham* [1904], who studied the case of a homogeneous soil layer bounded below by an impermeable boundary. He developed a solution to determine the air pressure at any depth in response to a periodic atmospheric pressure change at the ground surface. However, it was not until 6 decades later that the application of air flow in the vadose zone was proposed by R. W. Stallman. The work of *Stallman* [1967] and *Stallman and Weeks* [1969] at Badger Wash, near Cuba, New Mexico, demonstrated the use of observed air pressure variation in determining the permeability of the vadose zone material. In these field studies it was assumed that the vadose zone was homogeneous and underlain by an impermeable layer. Subsequently, *Weeks* [1978] applied the technique to determine air permeabilities for multilayer problems using a numerical approach.

Shan [1995] developed analytical solutions as an alternative tool for solving the one-dimensional air flow problem in multilayer seytems. *Rojstaczer and Tunks* [1995] conducted a field test study and determined the air diffusivity of a shallow, layered soil system using a one-dimensional analytical solution. Air permeabilities were later calculated using measured values of porosity and calculated values of diffusivity. Other analytical solutions are also available for solving air flow problems through axisymmetrical systems [*McWhorter*, 1990; *Baehr and Hult*, 1991; *Shan et al.*, 1992]. These solutions may be used in conjunction with appropriate field tests to estimate the air permeability of geologic materials in the vadose zone. Transport of gases in a fractured vadose zone was studied by *Nilson et al.* [1991], who assumed that the flow in the fracture is vertical and that the flow in the matrix is horizontal. Since the flow properties of a fault zone are usually quite different from those of the surrounding vadose zone material [*Mozley and Goodwin*, 1995; *Caine et al.*, 1996] the flow of air in the vicinity of the fault zone will be two-dimensional.

In this paper, analytical solutions are presented for a more realistic case where flow of air is assumed to be two-dimensional in the rock matrix and one-dimensional in the fault zone. The solutions are derived on the basis of the assumption of a sinusoidal type of atmospheric pressure variation at the ground surface. In reality, however, atmospheric pressure variations are rarely a sinusoidal function of time. Therefore a procedure is presented to extend the applicability of the solutions to an arbitrary atmospheric pressure variation. Examples are given to calculate the pressure variations in the vadose zone and to determine the air permeability of the fault zone using field data.

Paper number 1999WR900037.
0043-1397/99/1999WR900037$09.00

2. Theory

Let us consider a vertical fault cutting through a single layer of homogeneous, isotropic vadose zone. Figure 1 gives a cross section of such a system perpendicular to the fault zone, where $2b'$ and h' are the thicknesses of the fault zone and the vadose zone, respectively. A coordinate system has been chosen such that the x' axis is located on the ground surface and the z' axis is located vertically upward at one of the fault-rock interfaces. Considering an atmospheric pressure variation at the ground surface, we are interested in calculating the pressure variations at any arbitrary point in the subsurface. Because of the symmetric property of the system, the midplane of the fault zone may be considered a no-flow boundary. Therefore only one half of the system need be considered. In most cases the half width of the fault zone, b', is much smaller than either the horizontal dimension of the rock mass or the thickness of the system. This implies that flow through the fault zone may be assumed to be essentially one-dimensional with some lateral inflow from (or outflow to) the rock matrix. In the rock matrix at both sides of the fault zone the flow is two-dimensional on the cross-section plane. The governing equations for air flow in the rock matrix and the fault zone of the above system may be written as

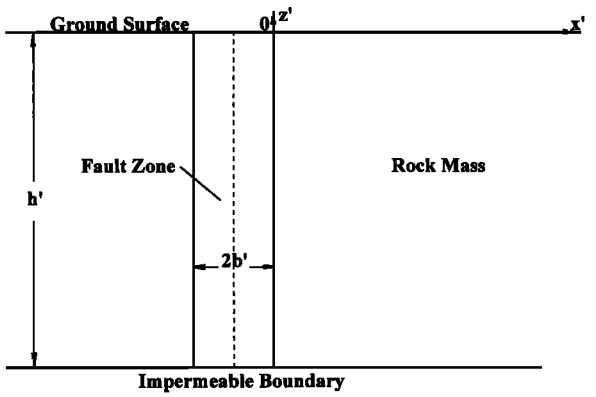

Figure 1. Schematic cross section of the fault zone and surrounding rocks.

$$\frac{\partial^2 \phi_r'}{\partial z'^2} + \frac{\partial^2 \phi_r'}{\partial x'^2} = \frac{1}{\alpha_r'} \frac{\partial \phi_r'}{\partial t'} \tag{1}$$

$$\frac{\partial^2 \phi_f'}{\partial z'^2} + \frac{1}{kb'} \left(\frac{\partial \phi_r'}{\partial x'} \right)_{x'=0} = \frac{1}{\alpha_f'} \frac{\partial \phi_f'}{\partial t'} \tag{2}$$

where the subscripts r and f are used to distinguish the rock mass terms from those of the fault zone; t' represents time; the pneumatic head ϕ' and the pneumatic diffusivity α' are defined by

$$\phi' = \frac{p}{\rho_m g} + z' \tag{3a}$$

$$\alpha' = \frac{k_a p_m}{n_a \mu_a} \tag{3b}$$

where p is air pressure (a variable); p_m and ρ_m are the mean air pressure and density (two constants), respectively; μ_a is the viscosity of air (a constant); k_a and n_a are air permeability and air-filled porosity, respectively (two constants but different for fault and rock); and g is the gravitational constant. In (2), k is the ratio of the air permeabilities of fault to rock, i.e.,

$$k = k_{af}/k_{ar} \tag{4}$$

We assume that $k > 1$, or in other words, the air permeability of the fault zone is larger than that of the rock mass. For cases where $k \leq 1$ (a relatively tight fault) the air flow in the vadose zone is one-dimensional, for which analytical solutions are available [*Shan*, 1995].

Equations (1) and (2) have been linearized by substituting the variable density ρ with its mean value ρ_m in mass flux derivation. This approximation is fairly accurate for problems of barometric pumping where the magnitude of pressure variation is relatively small [*Shan and Javandel*, 1999]. The initial condition used in this study is

$$\phi' = \phi_0' \tag{5}$$

where ϕ_0' is a constant.

The upper boundary condition is based on a sinusoidal variation of ϕ' at the land surface

$$\phi' = \phi_0' + \phi_a' \sin(\omega' t') \qquad z' = 0 \tag{6}$$

where ϕ_a' is a constant and ω' represents the frequency. Two kinds of lower boundary conditions are considered here:

$$\phi' = \phi_0' \qquad z' = -\infty \tag{7a}$$

$$\left(\frac{\partial \phi'}{\partial z'} \right) = 0 \qquad z' = -h' \tag{7b}$$

for large h' and small h', respectively.

To simplify the derivation and to generalize the problem, we introduce the following dimensionless variables and parameters:

$$\phi = \frac{\phi' - \phi_0'}{\phi_a'} \tag{8a}$$

$$x = \frac{x'}{b'} \qquad z = \frac{z'}{b'} \qquad h = \frac{h'}{b'} \tag{8b}$$

$$t = \frac{\alpha_r' t'}{b'^2} \qquad n = \frac{n_{af}}{n_{ar}} \qquad \alpha = \frac{\alpha_f'}{\alpha_r'} = \frac{k}{n} \qquad \omega = \frac{b'^2 \omega'}{\alpha_r'} \tag{8c}$$

The substitutions of (8a)–(8c) into (1) and (2) lead to the dimensionless governing equations:

$$\frac{\partial^2 \phi_r}{\partial z^2} + \frac{\partial^2 \phi_r}{\partial x^2} = \frac{\partial \phi_r}{\partial t} \tag{9}$$

$$\frac{\partial^2 \phi_f}{\partial z^2} + \frac{1}{k} \left(\frac{\partial \phi_r}{\partial x} \right)_{x=0} = \frac{1}{\alpha} \cdot \frac{\partial \phi_f}{\partial t} \tag{10}$$

The dimensionless formulae also reduce the initial and boundary conditions to

$$\phi_r(x, z, 0) = \phi_f(z, 0) = 0 \tag{11}$$

$$\phi_r(x, 0, t) = \phi_f(0, t) = \sin(\omega t) \tag{12}$$

$$\phi_r(x, -\infty, t) = \phi_f(-\infty, t) = 0 \tag{13a}$$

$$\left(\frac{\partial \phi_r}{\partial z} \right) = \left(\frac{\partial \phi_f}{\partial z} \right) = 0 \qquad z = -h \tag{13b}$$

To solve (9) and (10), we also need to use the inner boundary condition at the fault-rock interface where the pneumatic head is continuous:

$$\phi_r(0, z, t) = \phi_f(z, t) \tag{14}$$

Note that (13a) and (13b) represent two different lower boundary conditions: the former maintains a constant (unaffected initial) pneumatic head at an infinite depth, and the latter constitutes a gas-impermeable boundary (water table or bed rock) at a finite depth. For brevity we only present the solutions here. Details of derivation are given by *Shan* [1990].

2.1. Case 1: Vadose Zone With Semi-infinite Thickness

In this case the solution for the dimensionless pneumatic head in the rock mass is

$$\phi_r = e^{z\sqrt{\omega/2}} \sin(\omega t + z\sqrt{\omega/2}) - \frac{2\omega}{\pi} \int_0^\infty \frac{u e^{-u^2 t} \sin(uz)}{\omega^2 + u^4} du$$

$$+ \omega \int_0^t \operatorname{erfc}\left(\frac{x}{2\sqrt{\tau}} \right) \left[1 - \operatorname{erfc}\left(\frac{-z}{2\sqrt{\tau}} \right) \right] \cos[\omega(t$$

$$- \tau)]\, d\tau - \frac{2(\alpha - 1)\omega}{\pi} \int_0^\infty \sin(\rho z)\, d\rho \int_0^t [f_1(x, \rho, \tau) + f_2(x, \rho, \tau)] \cos[\omega(t - \tau)]\, d\tau \quad (15)$$

where erfc(u) is the complementary error function and the two functions in the integrand are defined by

$$f_1(x, \rho, t) = \frac{\rho}{B_1(B_1 - B_2)} \exp(B_1 x + B_1^2 t - \rho^2 t) \cdot \operatorname{erfc}\left(B_1\sqrt{t} + \frac{x}{2\sqrt{t}}\right) \quad (16a)$$

$$f_2(x, \rho, t) = \frac{-\rho}{B_2(B_1 - B_2)} \exp(B_2 x + B_2^2 t - \rho^2 t) \cdot \operatorname{erfc}\left(B_2\sqrt{t} + \frac{x}{2\sqrt{t}}\right) \quad (16b)$$

Parameters B_1 and B_2 are defined by

$$B_1, B_2 = \frac{1}{2}\left(\frac{1}{n} \pm \sqrt{\Delta}\right) \qquad \Delta > 0 \quad (17a)$$

$$B_1, B_2 = \frac{1}{2}\left(\frac{1}{n} \pm i\sqrt{-\Delta}\right) \qquad \Delta < 0 \quad (17b)$$

where the positive sign applies to B_1 and the negative sign corresponds to B_2; the discriminant, Δ is defined as

$$\Delta = \frac{1}{n^2} - 4(\alpha - 1)\rho^2 \quad (18)$$

To obtain the solution for ϕ_f, one may simply set $x = 0$ in the solution for ϕ_r. It is interesting to note that the sum of the first two terms in (15) is the solution for one-dimensional vertical air flow. Also note that as $x \to \infty$, the other two terms vanish, and (15) is reduced to the one-dimensional solution. To calculate the integral in (15), we have first to determine which equation ((17a) or (17b)) should be used to calculate B_1 and B_2. Noting that n and α refer to the air-filled porosity ratio and the diffusivity ratio of the fault to the rock, respectively, both terms must have positive values. It is then easy to see that (17a) should always be used whenever $\alpha \leq 1$ (Δ is positive). For cases when $\alpha > 1$, which is the case of interest to us, we need to calculate the integral in (15) in two parts, from 0 to ρ_0 and from ρ_0 to ∞, using (17a) and (17b), respectively. The critical value of ρ is defined by

$$\rho_0 = \frac{1}{2n\sqrt{\alpha - 1}} \qquad \alpha > 1 \quad (19)$$

More discussion on calculating the integral using (17b) is given by *Shan* [1990].

2.2. Case 2: Vadose Zone Bounded Below by Gas-Impermeable Boundary

In this case the solution for the dimensionless pneumatic head in the rock mass is

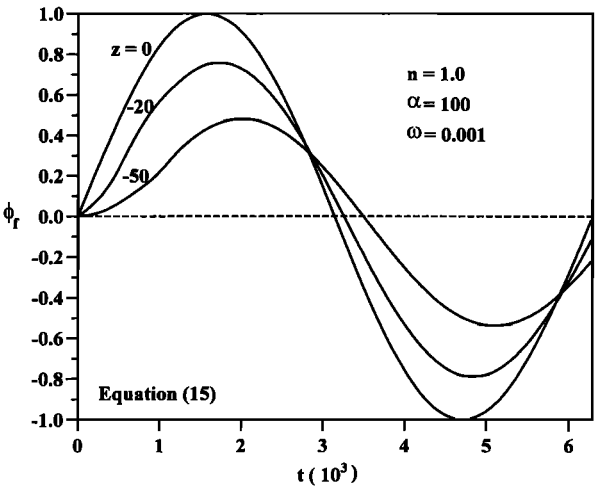

Figure 2a. Variation of dimensionless pneumatic head in the fault zone at three different depths.

$$\phi_r = \frac{2\omega}{h}\left[-\frac{\sin(\omega t)}{\omega}\sum_{m=1}^{\infty}\frac{d^3 \sin(dz)}{d^4 + \omega^2} + \cos(\omega t)\sum_{m=1}^{\infty}\frac{d \sin(dz)}{d^4 + \omega^2} - \sum_{m=1}^{\infty}\frac{de^{-d^2 t}\sin(dz)}{d^4 + \omega^2}\right] - \frac{2(\alpha - 1)\omega}{h}\sum_{m=1}^{\infty}\sin(dz)\int_0^t [f_1(x, d, \tau) + f_2(x, d, \tau) + f_3(x, d, \tau)]\cos[\omega(t - \tau)]\, d\tau \quad (20)$$

where

$$d = \left(m - \frac{1}{2}\right)\frac{\pi}{h} \quad (21)$$

and m is a positive integer. In (20), f_1 and f_2 are defined by (16a) and (16b), respectively, while f_3 is defined by

$$f_3(x, d, t) = \frac{1}{d(\alpha - 1)} e^{-d^2 t} \operatorname{erfc}\left(\frac{x}{2\sqrt{t}}\right) \quad (22)$$

As $x \to \infty$, the second term in (20) vanishes, and the solution is reduced to a one-dimensional solution.

3. Results

To examine the effect of the permeability contrast between the fault zone and the surrounding rocks and for the sake of simplicity, we assume an equal air-filled porosity for the fault and the rock mass. As a result, the permeability ratio k would be the same as the diffusivity ratio α. We also assume that the permeability of the rock mass has been determined.

Calculated by using the analytical solution for case 1 (Equation (15)), Figures 2a, 2b, and 3 illustrate how a sinusoidal signal propagates in a semi-infinite system. We used a dimensionless frequency $\omega = 0.001$ in Figures 2a, 2b, and 3 and set $k = \alpha = 100$ in Figures 2a and 2b to calculate the dimensionless pneumatic head in the fault zone and the rock mass, respectively. Figure 2a shows results for the variation of dimensionless pneumatic head at the land surface and at differ-

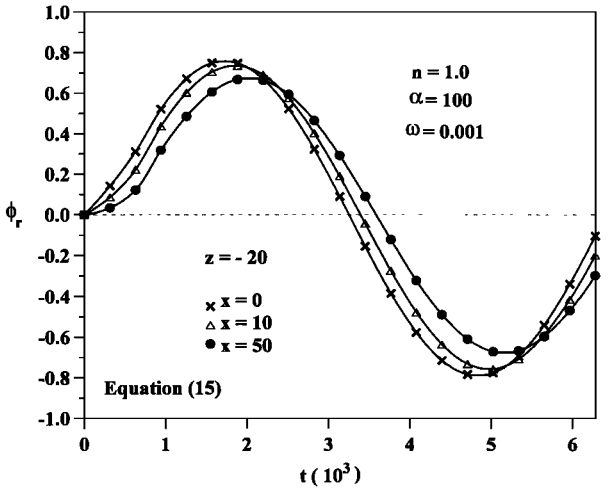

Figure 2b. Variation of dimensionless pneumatic head at dimensionless depth $z = -20$ in the rock mass for three different locations.

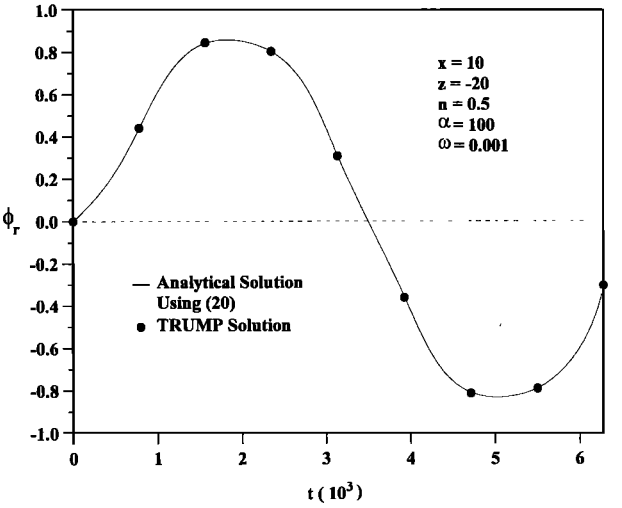

Figure 4. Comparison of analytical solution with numerical (TRUMP) solution.

ent depths in the fault zone. The amplitude of the head variation decreases with depth, while the "period" of the head variation increases with depth. For any given system a practical depth exists below which the head variation is insignificant (e.g., $z < -200$ for the fault zone in Figure 2a). Figure 2b shows results at three different points, $x = 0$, 10, and 50 at a depth of $z = -20$, using the same parameters as were used in Figure 2a. Under the given conditions the closer the point of observation is to the fault zone at a given depth, the quicker and larger the response to a pressure variation at the land surface. To study the effect of the permeability (diffusivity) ratio, we calculated the dimensionless pneumatic pressure variations at a point $x = 10$ and $z = -20$ using four different α values. Note that $\alpha = 1$ represents the solution for one-dimensional problems. The results are shown in Figure 3, which illustrates how a large fault zone diffusivity (permeability) leads to an increase in the pneumatic head variation.

It is well known that the significance of analytical solutions is twofold: (1) direct application to practical problems and (2) application to verifying a numerical code. We chose a well-established code, TRUMP [*Edwards*, 1972], for the purpose of verification. A faulted vadose zone with a dimensionless thickness of $h = 100$ is taken into consideration. The other parameters assumed for this calculation are $n = 0.5$, $\alpha = 100$, and $\omega = 0.001$. For the numerical simulation a uniform grid size of 1 was used in the z direction; the element size in the x direction was designed to increase by doubling, i.e., 1, 2, 4, 8, 16, 32, and 64, where 1 is the width of all the fault elements and the others are the widths of the rock elements. In Figure 4 the TRUMP solution is compared with the corresponding analytical solution (equation (20), the solid line) at the point $x = 10$ and $z = -20$, and they show excellent agreement.

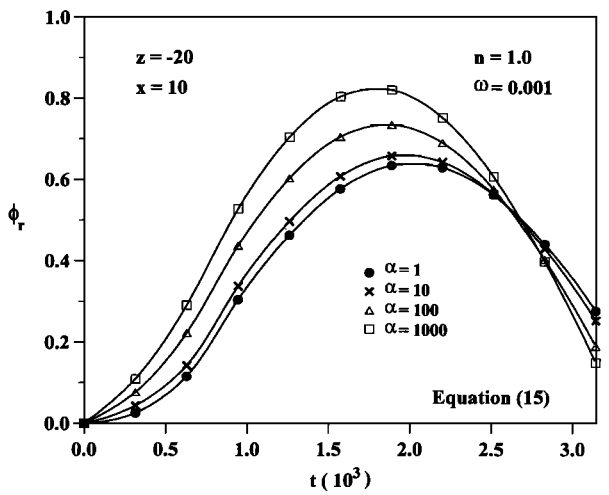

Figure 3. Effect of diffusivity contrast on the variation of dimensionless pneumatic head at the point $x = 10$ and $z = -20$.

On one hand, the analytical solution can be used to verify the numerical code; on the other hand, the verified code may be used to check the validity of assumptions that are the basis for the analytical solutions. An assumption specifically introduced in this study is that of one-dimensional vertical flow in the fault zone. The validity of this assumption can be checked by means of TRUMP because, as a numerical code, TRUMP can be used to simulate a model that allows two-dimensional flow in both the rock mass and the fault zone. Actually, this can be done by dividing the fault zone into several elements along the horizontal direction (x direction) as well as along the vertical direction (z direction). In this way the pneumatic head distribution in the fault zone along the horizontal direction is also calculated. Calculation results for a wide range of parameter combinations have revealed that except for very small values of time and permeability contrast the assumption of one-dimensional flow in the fault zone is quite reasonable [*Shan*, 1990].

4. Applications

4.1. Procedure for Practical Applications

The solutions presented earlier were developed for a simple sinusoidal pressure variation at the land surface. They can, however, be applied to any arbitrary atmospheric pressure variations using the Fourier series theory as discussed below.

1. Assuming the observed atmospheric pressure variation is expressed by $p'(t')$ and the initial pressure is p_0, calculate

Table 1. Parameters Used for Calculations

Parameter	Value
t'_m, hours	24
p_0, cm water	942.02
p_m, cm water	944.5
b', m	1.0
n_{af}	0.1
n_{ar}	0.1
T, °C	15

the variation of pneumatic head at the land surface: $\phi'(t') = [p'(t') - p_0]/\rho_m g$. This implies that $\phi'_0 = 0$.

2. Let t'_m represent the maximum study time. Calculate the Fourier expansion for $\phi'(t')$ using

$$\phi'(t') = \sum_{i=1}^{\infty} \phi_{i'}(t') = \sum_{i=1}^{\infty} \phi_{a'i} \sin(\omega_i t') \tag{23a}$$

where

$$\phi_{a'i} = \frac{2}{t_{m'}} \int_0^{t_{m'}} \phi'(t') \sin(\omega_i t')\, d't \tag{23b}$$

$$\omega'_i = \frac{\pi i}{t'_m} \tag{23c}$$

3. Calculate the ratio of air-filled porosity n, the ratio of pneumatic diffusivity α, and the maximum dimensionless time t_m using (8c).

4. For each term $\phi'_i(t')$ in (23a), calculate its corresponding dimensionless frequency ω_i using (8c).

5. For a given point (x, z) and a given time t calculate the dimensionless ϕ_{ri} using (15). The corresponding dimensional term can be easily obtained by multiplying ϕ_{ri} by a factor of ϕ'_{ai}.

6. Add all the solutions, each of which corresponds to an individual term of (23a), to obtain the variation of pneumatic head at the given location and time, $\phi'(x, z, t)$.

4.2. Application Examples

We took the atmospheric pressure variation recorded at Tucson, Arizona [*Shan*, 1995], to illustrate the application of the method presented above. Some parameters used for the calculations are given in Table 1. In step 2 the Fourier coefficients given by (23b) were calculated using the following equations [*Shan*, 1995]:

$$\phi'_{ai} = \frac{2}{t'_m} \sum_{j=1}^{N-1} \left\{ \frac{c_j}{\omega'^2_i} [\sin(\omega'_i t'_{j+1}) - \sin(\omega'_i t'_j)] + \frac{c_j t'_j + d_j}{\omega'_i} \cos(\omega'_i t'_j) - \frac{c_j t'_{j+1} + d_j}{\omega'_i} \cos(\omega'_i t'_{j+1}) \right\} \tag{24}$$

where N is the number of data points (in this example, $N = 49$) and the two coefficients are defined by

$$c_j = (\phi'_{j+1} - \phi'_j)/(t'_{j+1} - t'_j) \tag{25a}$$

$$d_j = (\phi'_j t'_{j+1} - \phi'_{j+1} t'_j)/(t'_{j+1} - t'_j) \tag{25b}$$

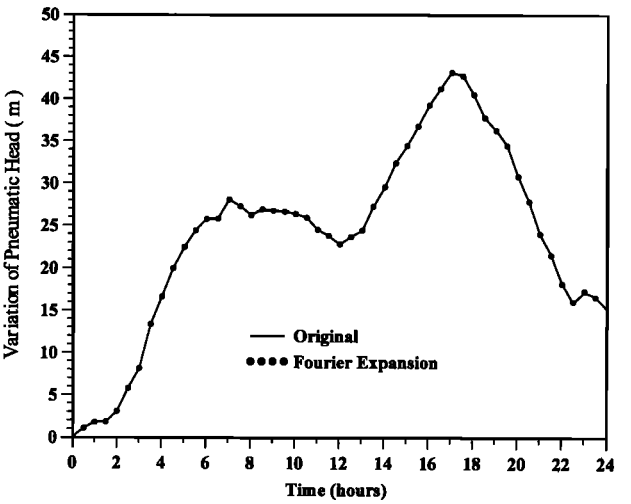

Figure 5. A comparison of the observed pneumatic head variation and its Fourier series expansion.

A comparison between the observed pneumatic head variation and its Fourier expansion with 500 terms is given in Figure 5. A maximum relative error of ~1% was found at data points close to the two ends of the time domain (0 and 24 hours). For other data points the relative error is much smaller than 1%.

Three cases were considered. In the first case, assumed air permeabilities of $k_{ar} = 10^{-12}$ m^2 and $k_{af} = 10^{-11}$ m^2 were used to calculate the variations of pneumatic head at five points. The results at three different depths (10, 20, and 30 m) in the fault zone are compared with the variation of pneumatic head at the land surface in Figure 6a. A comparison of the calculated head variations at the depth of 10 m and distances of 0, 10, and 20 m from the fault zone is given in Figure 6b. There is a significant pneumatic head change with depth as shown in Figure 6a. However, at a given depth ($z' = -10$ m) the pneumatic head variation with the distance from the fault zone is not very distinctive (Figure 6b). The slight change of pneumatic head in the horizontal direction is caused by the

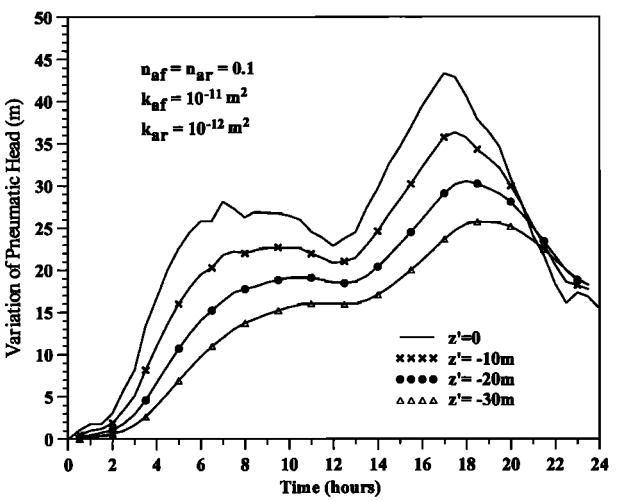

Figure 6a. Calculated pneumatic head variation at three different depths in the fault zone for the case of a permeability contrast of 10.

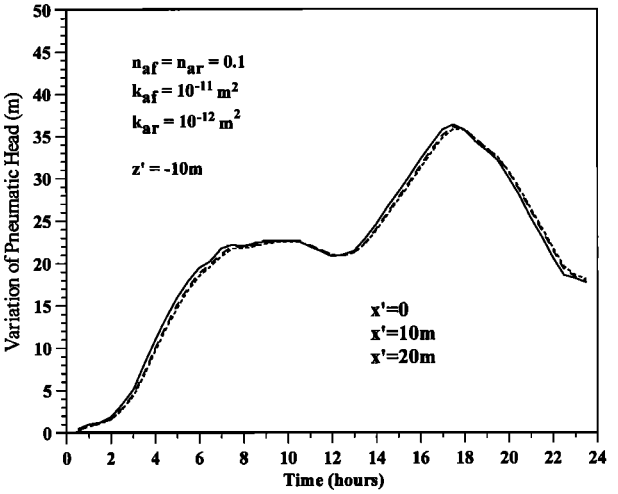

Figure 6b. Calculated pneumatic head variation at three different locations in the rock mass at the depth of 10 m for a permeability contrast of 10 and $k_{ar} = 10^{-12}$ m^2.

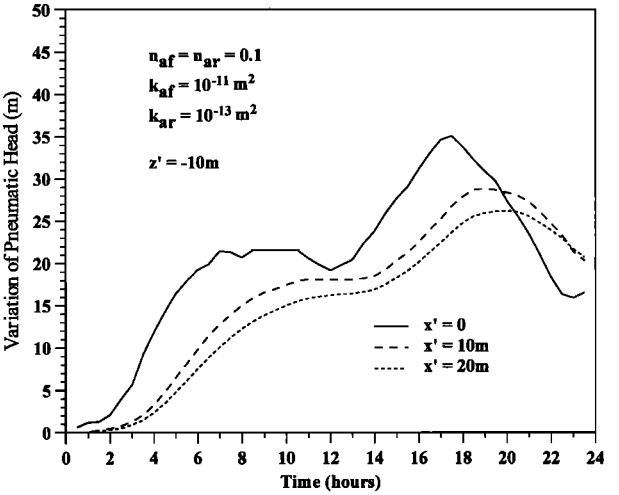

Figure 8. Calculated pneumatic head variation at three different locations in the rock mass at the depth of 10 m for a permeability contrast of 100 and $k_{ar} = 10^{-13}$ m^2.

horizontal flow component that is affected both by the contrast of permeabilities and by their absolute values.

In the second case both permeabilities were lowered by 1 order of magnitude, i.e., $k_{ar} = 10^{-13}$ m^2 and $k_{af} = 10^{-12}$ m^2, and the variations of pneumatic head were calculated at the same points as in Figure 6b for case 1. As is shown in Figure 7, the head change in the horizontal direction is larger than that in Figure 6b, where both the rock mass and the fault zone are very permeable.

In the third case the air permeability of the rock mass was kept the same as in case 1, but the air permeability for the fault zone was increased by 1 order of magnitude. As indicated in Figure 8, the head change in the horizontal direction is even larger when the permeability contrast increases. The effect of permeability contrast (or the effect of fault zone) on the variation of pneumatic head decreases with the increase of distance from the fault. Therefore the permeability of the rock mass can be determined using data observed at a long distance (e.g., 50 m for the above cases) away from the fault zone.

As a hypothetical example, let us assume that the air permeability of the rock mass has been determined as $k_{ar} = 10^{-12}$ m^2 and that the variation of pneumatic head has been observed at a depth of 10 m in the fault zone (see the dots in Figure 9). Using the method of trial and error, a value was assigned to the air permeability for the fault zone, the variation of pneumatic head at the observation point was calculated, and the result was compared with the observation data. The process was repeated until the best match was achieved. For this example we found that a fault zone air permeability of 10^{-10} m^2 gave the best fit with the observation data, as shown in Figure 9.

In any practical applications, for the purpose of satisfying the assumption of an initially no-flow condition, one should choose $t' = 0$ at a time when the pneumatic head at the land surface and at depths are approximately the same. In the field study by *Weeks* [1978] this time is 10 or 11 A.M.

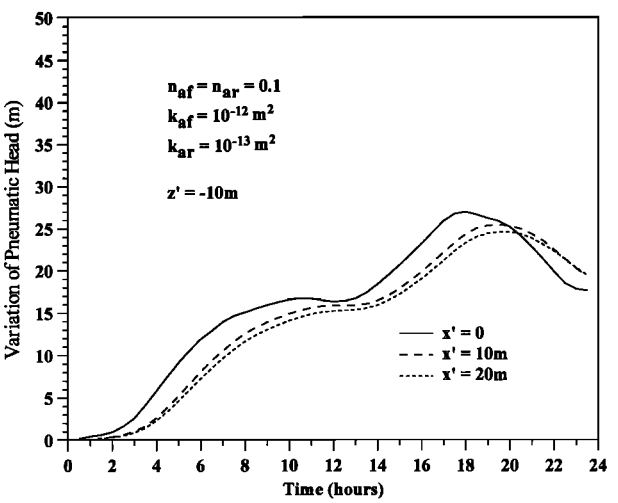

Figure 7. Calculated pneumatic head variation at three different locations in the rock mass at the depth of 10 m for a permeability contrast of 10 and $k_{ar} = 10^{-13}$ m^2.

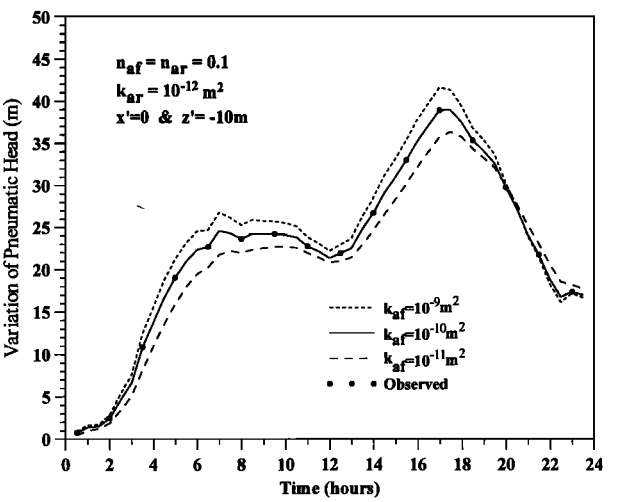

Figure 9. Calculated pneumatic head variation at $x' = 0$ and $z' = -10$ m for three different permeability contrasts.

5. Conclusions

Analytical solutions for gas flow in a faulted vadose zone were presented. Although these solutions were derived for a simple sinusoidal boundary condition, a procedure was also introduced to apply them to field problems with arbitrary atmospheric pressure variations at ground surface. Using field-measured atmospheric pressure data and assumed system parameters, the variations of pneumatic head at different locations in a hypothetical system were calculated. A sensitivity study showed that variations of pneumatic head (or pressure) in the subsurface may be affected by both the air permeability contrast of fault zone to rock mass and the absolute permeability values. Finally, an example was given to show the applicability of the solutions in determining the air permeability of the fault zone using field data. In deriving the above solutions it was assumed that the air flow in the rock mass and the fault zone were two- and one-dimensional, respectively.

Acknowledgments. This work was done at the Lawrence Berkeley National Laboratory, which is operated by the University of California for the U.S. Department of Energy under Contract DE-AC03-76SF00098. The authors thank G. J. Moridis for reviewing the manuscript.

References

Baehr, A. L., and M. F. Hult, Evaluation of unsaturated zone air permeability through pneumatic tests, *Water Resour. Res.*, *27*(10), 2605–2617, 1991.

Buckingham, E., Contributions to our knowledge of the aeration of soils, *Soils Bur. Bull.*, *25*, U.S. Dep. of Agric., Washington, D. C., 1904.

Caine, J. S., J. P. Evans, and C. B. Forster, Fault zone architecture and permeability structure, *Geology*, *24*(11), 1025–1028, 1996.

Edwards, A. L., TRUMP: A computer program for transient and steady state temperature distribution in multidimensional systems, *Rep. UCRL-14754*, Lawrence Livermore Natl. Lab., Livermore, Calif., 1972.

McWhorter, D. B., Unsteady radial flow of gas in the vadose zone, *J. Contam. Hydrol.*, *5*, 297–314, 1990.

Mozley, P. S., and L. B. Goodwin, Patterns of cementation along a Cenozoic normal fault: A record of paleoflow orientations, *Geology*, *23*(6), 539–542, 1995.

Nilson, R. H., E. W. Peterson, K. H. Lie, N. R. Burkhard, and J. R. Hearst, Atmospheric pumping: A mechanism causing vertical transport of contaminated gases through fractured permeable media, *J. Geophys. Res.*, *96*(13), 21,933–21,948, 1991.

Rojstaczer, S., and J. P. Tunks, Field-based determination of air diffusivity using soil air and atmospheric pressure time series, *Water Resour. Res.*, *31*(12), 3337–3343, 1995.

Shan, C., *Characterization of Leaky Faults*, Ph.D. dissertation, Univ. of Calif., Berkeley, 1990.

Shan, C., Analytical solutions for determining vertical air permeability in unsaturated soils, *Water Resour. Res.*, *31*(9), 2193–2200, 1995.

Shan, C., and I. Javandel, Approximate equations for gas flow through porous media, *Rep. LBNL-42780*, Lawrence Berkeley Natl. Lab., Univ. of Calif., Berkeley, 1999.

Shan, C., R. W. Falta, and I. Javandel, Analytical solutions for steady state gas flow to a soil vapor extraction well, *Water Resour. Res.*, *28*(4), 1105–1120, 1992.

Stallman, R. W., Flow in the zone of aeration, *Adv. Hydrosci.*, *4*, 151–195, 1967.

Stallman, R. W., and E. P. Weeks, The use of atmospherically induced gas-pressure fluctuations for computing hydraulic conductivity of the unsaturated zone (abs.), *Geol. Soc. Am. Abstr. Programs*, *7*, 213, 1969.

Weeks, E. P., Field determination of vertical permeability to air in the unsaturated zone, *U.S. Geol. Surv. Prof. Pap.*, *1051*, 41, 1978.

I. Javandel, C. Shan, and P. Witherspoon, Earth Sciences Division, Lawrence Berkeley National Laboratory, One Cyclotron Road, MS 90-1116, Berkeley, CA 94720. (c_shan@lbl.gov)

(Received August 28, 1998; revised February 2, 1999; accepted February 3, 1999.)